

Hydrogen Storage in Microporous Titanium Oxides Reduced by Early Transition Metal Organometallic Sandwich Compounds

Xin Hu,[†] Michel Trudeau,[‡] and David M. Antonelli^{*,†}

Department of Chemistry and Biochemistry, University of Windsor, Windsor, Ontario N9B 3P4, Canada,
Chemistry and Materials, Hydro-Québec Research Institute, Varennes, Quebec J3X 1S1, Canada

Received December 11, 2006. Revised Manuscript Received January 12, 2007

Microporous titanium oxides synthesized using a hexylamine template were reduced by excess bis(benzene) chromium, bis(cyclopentadienyl) chromium, bis(benzene) vanadium, and bis(cyclopentadienyl) vanadium. These new composite materials were characterized by nitrogen adsorption, powder X-ray diffraction, X-ray photoelectron spectroscopy, and elemental analysis. The V and Cr sandwich compounds proved less effective in reducing the Ti oxide surface than bis(toluene) titanium, which was studied previously. The hydrogen sorption properties were measured at 77 K. The gravimetric sorption capacity decreased in each case as compared to that of the unreduced sample, possibly due to increased density or the reduced surface areas after reduction. However, the overall volumetric storage capacities increased, with a high of 33.42 kg/m³ recorded for the bis(benzene) vanadium reduced material at 100 atm. This is less than that previously obtained for bis(toluene) titanium (40.46 kg/m³). The improved performance of this series of composite materials relative to the untreated sample was attributed to the increased reduction level of the metal centers in the framework of the structure, which allows for more facile π -back-donation to the H–H σ -bond. Unlike MOFs and porous carbons, the performance does not depend greatly on surface area. Maximum H₂ binding enthalpies ranging from 4.57 to 8.35 kJ/mol were calculated for all samples. The increasing enthalpies with hydrogen adsorption capacity are consistent with a different adsorption mechanism than physisorption, possibly involving a Kubas-type interaction. These results indicate that further efforts are required to find a suitable reducing reagent in order to reach even higher volumetric storage densities and tune the hydrogen binding enthalpies to over 15 kJ/mol, which is proposed to be ideal for porous samples operating at ambient temperature.

Introduction

The demand for an efficient and clean fuel alternative has increased in the past decade and is expected to become more pronounced in the future, as fossil fuel providence will become increasingly limited. Hydrogen represents an ideal alternative as a fuel because it is abundant,¹ can readily be synthesized electrochemically, and when used in a fuel cell with oxygen produces only water as a byproduct, i.e., it is environmentally friendly. However, the main concern to date is the safe and efficient transport of this extremely flammable gas. To overcome this problem, we may use solids that adsorb hydrogen at lower pressure as carriers, thus avoiding the cumbersome storage vessels required for high pressure containment. The major requirements for alternative hydrogen storage materials are: fast kinetics near ambient temperature, low density, high gravimetric/volumetric capacity, and high tolerance for recycling. Many metals² and metal hydride alloys³ have been studied. These solids adsorb between 2 and 7 wt % hydrogen between 100 and 200 °C.⁴ Because the U.S. Department of Energy (DOE) has defined

9 wt % as a 2015 system target for gravimetric hydrogen storage, these materials have so far fallen short of expectations. Advances in materials synthesis have led to the development of carbon-based nanostructured materials,^{5–14} zeolites,^{15–20} and microporous metal–organic frameworks

* To whom correspondence should be addressed. E-mail: danton@uwindsor.ca.
[†] University of Windsor.

[‡] Hydro-Québec Research Institute.

(1) Schlapbach, L.; Züttel, A. *Nature* **2001**, *414*, 353.

(2) Yartys, V. A.; Harris, I. R.; Panasyuk, V. V. *Mater. Sci.* **2001**, *37*, 219.

(3) Sandrock, G. A. *J. Alloys Compd.* **1999**, *293–295*, 877.

(4) Seayad, A. M.; Antonelli, D. M. *Adv. Mater.* **2004**, *16*, 765.

(5) Dillon, A. C.; Jones, K. M.; Bekkedahl, T. A.; Kiang, C. H.; Bethune, D. S.; Heben, M. J. *Nature* **1997**, *386*, 377.

(6) Chen, P.; Wu, X.; Lin, J.; Tan, K. L. *Science* **1999**, *285*, 91.

(7) Ye, Y.; Ahn, C. C.; Witham, C.; Fultz, B.; Liu, J.; Rinzler, A. G.; Colbert, D.; Smith, K. A.; Smalley, R. E. *Appl. Phys. Lett.* **1999**, *74*, 2307.

(8) Liu, C.; Fan, Y. Y.; Liu, M.; Cong, H. T.; Cheng, H. M.; Dresselhaus, M. S. *Science* **1999**, *286*, 1127.

(9) Poirier, E.; Chahine, R.; Benard, P.; Cossement, D.; Lafi, L.; Melancon, E.; Bose, T. K.; Deilets, S. *Appl. Phys. A: Mater. Sci. Process.* **2004**, *78*, 961.

(10) Tibbetts, G. G.; Meisner, G. P.; Olk, C. H. *Carbon* **2001**, *39*, 2291.

(11) Nijkamp, M. G.; Raaymakers, J. E. M. J.; van Dillen, A. J.; de Jong, K. P. *Appl. Phys. A: Mater. Sci. Process.* **2001**, *72*, 619.

(12) Schimmel, H. G.; Kearley, G. J.; Nijkamp, M. G.; Visser, C. T.; de Jong, K. P.; Mulder, F. M. *Chem.—Eur. J.* **2003**, *9*, 4764.

(13) Benard, P.; Chahine, R. *Langmuir* **2001**, *17*, 950.

(14) Zuttel, A.; Sudan, P.; Mauron, P.; Emmenegger, S.; Schlapbach, L. *Int. J. Hydrogen Energy* **2002**, *27*, 203.

(15) Zecchina, A.; Bordiga, S.; Vitillo, J. G.; Ricchiardi, G.; Lamberti, C.; Spoto, G.; Bjorgen, M.; Lillerud, K. P. *J. Am. Chem. Soc.* **2005**, *127*, 6361.

(16) Arean, C. O.; Delgado, M. R.; Palomino, G. T.; Rubio, M. T.; Tsyganenko, N. M.; Tsyganenko, A. A.; Garrone, E. *Microporous Mesoporous Mater.* **2005**, *80*, 247.

(17) Langmi, H. W.; Walton, A.; Al-Mamouri, M. M.; Johnson, S. R.; Book, D.; Speight, J. D.; Edwards, P. P.; Gameson, I.; Anderson, P. A.; Harris, I. R. *J. Alloys Compd.* **2003**, *356–357*, 710.

(18) Kazansky, V. B.; Borovkov, V. Y.; Serich, A.; Karge, H. G. *Microporous Mesoporous Mater.* **1998**, *22*, 251.

(MOFs)^{21–32} for room temperature or cryogenic hydrogen storage. This latter method of storage is of some practical interest because the technology needed for transportation of large quantities of liquid hydrogen already exists in the rocket industry. Some of these materials have shown promising hydrogen uptake;^{7,26} however, there is yet no report of any material meeting or surpassing the 2015 DOE target values.

Recent advances within our group indicated that micro- and mesoporous Ti oxides could serve as hosts for hydrogen storage.⁴ Micro- and mesoporous Ti oxides are in many ways ideal candidates for hydrogen storage because they can be made from inexpensive and light metal Ti, and the surface area, pore size, and wall thickness can be systematically controlled.³³ Micro- and mesoporous oxides can also be synthesized on a kilogram scale and the variable oxidation states of the Ti center,³⁴ a feature not present in MOFs, zeolites, or porous carbon, may also offer further advantages because binding of H₂ to transition metals is strongly dependent on the electron density at the metal center and its ability to back-bond through a π -interaction into the anti-bonding H–H orbital.^{35,36} Calculations by Zhao et al. have predicted high storage capacities and ideal enthalpies of 20–30 kJ/mol for hypothetical Sc- and Ti-modified C₆₀ moieties on the basis of binding of the H–H σ -bond to the metal center.³⁶ Similar calculations predict that low-coordinate, low-valence Ti centers grafted onto carbon nanotubes should also improve storage capacities and binding enthalpies.³⁷ In line with these predictions, microporous Ti oxide treated with bis(toluenes) Ti, a chemical that deposits low-valence Ti on the surface, possesses a gravimetric storage capacity at 77 K and 100 atm of close to 5 wt % with a volumetric storage capacity of 40.46 kg/m³.³⁸ This is the highest volumetric reported for any cryogenic storage material we know of.

Although gravimetric capacity is often a major target for research in H₂ storage materials, there are practical limits associated with the tank volume required to house the adsorbent, which makes volumetric capacity just as important, and in some sense even more important, a parameter to consider. Reduction of the microporous Ti oxide surface also leads to a dramatic change in the enthalpy properties, resulting in higher enthalpies of adsorption, which increase on hydrogen loading, suggesting a different mechanism than simple physisorption, possibly involving a Kubas-type interaction. However, to verify this, more experimentation is necessary. In previous reports, we showed that mesoporous Nb oxide can act as a potent stoichiometric electron acceptor.³⁹ Although alkali metals are capable of reducing the framework by a total of one oxidation state without loss of the mesostructure,⁴⁰ organometallic reductants such as bis(benzene) chromium, bis(cyclopentadienyl) chromium, bis(benzene) vanadium, and bis(cyclopentadienyl) vanadium, deposit transition metal atoms on the surface or leave mixed-oxidation-state phases within the pores of the structure, depending on the compound.^{41–43} Because these compounds act as reducing agents and leave low-valent transition metal residues behind, which themselves may serve as binding sites for H₂, it stands to reason that they may function as useful dopants to improve the hydrogen-storage performance of microporous Ti oxides. Herein, we synthesize and investigate the hydrogen-sorption properties of bis-arene and bis-cyclopentadienyl transition-metal-reduced microporous titanium oxide composites in order to exploit the reducible nature of the surface to tune the binding enthalpies and hydrogen storage capacity.

Experimental Section

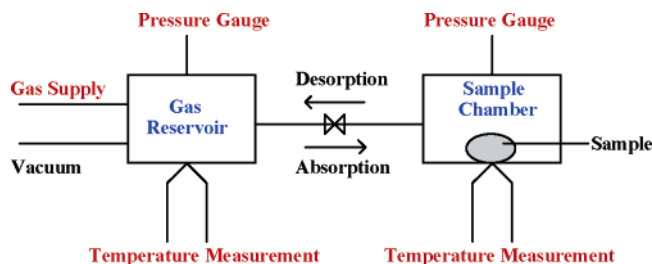
Materials and Equipment. All chemicals unless otherwise stated were obtained from Aldrich. Bis(benzene) chromium, bis(cyclopentadienyl) chromium, and bis(cyclopentadienyl) vanadium were obtained from Strem. Bis(benzene) vanadium was prepared according to the literature.⁴⁴ Nitrogen adsorption and desorption data were collected on a Micromeritics ASAP 2010. X-ray diffraction (XRD) patterns (Cu K α) were recorded in a sealed glass capillary on a Siemens D-500 θ – 2θ diffractometer. All X-ray photoelectron spectroscopy (XPS) peaks were referenced to the carbon C–(C, H) peak at 284.8 eV, and the data were obtained using a Physical Electronics PHI-5500 spectrometer using charge neutralization. All elemental analysis data (conducted under an inert atmosphere) were obtained from Galbraith Laboratories, Knoxville, TN.

H₂ Sorption Measurements. The hydrogen adsorption/desorption isotherms have been measured by a computer-controlled commercial Gas Reaction Controller manufactured by the Advanced Materials Corporation of Pittsburgh, PA. Highly purified hydrogen (99.9995% purity) was used as the adsorbent. Typically, the mass required for the hydrogen sorption measurement is 500–1000 mg.

- (19) Vitillo, J. G.; Ricchiardi, G.; Spoto, G.; Zecchina, A. *Phys. Chem. Chem. Phys.* **2005**, *7*, 3948.
- (20) Langmi, H. W.; Book, D.; Walton, A.; Johnson, S. R.; Al-Mamouri, M. M.; Speight, J. D.; Edwards, P. P.; Harris, I. R.; Anderson, P. A. *J. Alloys Compd.* **2005**, *404–406*, 637.
- (21) Rosi, N. L.; Eckert, J.; Eddoudi, M.; Vodak, D. T.; Kim, J.; O’Keeffe, M.; Yaghi, O. M. *Science* **2003**, *300*, 1127.
- (22) Rowsell, J. L. C.; Milward, A. R.; Park, K. S.; Yaghi, O. M. *J. Am. Chem. Soc.* **2004**, *126*, 5666.
- (23) Rowsell, J. L. C.; Yaghi, O. M. *Angew. Chem., Int. Ed.* **2005**, *44*, 4670.
- (24) Panella, B.; Hirscher, M. *Adv. Mater.* **2005**, *17*, 538.
- (25) Kaye, S. S.; Long, J. R. *J. Am. Chem. Soc.* **2005**, *127*, 6506.
- (26) Wong-Foy, A. G.; Matzger, A. J.; Yaghi, O. M. *J. Am. Chem. Soc.* **2006**, *128*, 3494.
- (27) Zhao, X.; Xiao, B.; Fletcher, A. J.; Thomas, K. M.; Bradshaw, D.; Rosseinsky, M. J. *Science* **2004**, *306*, 1012.
- (28) Dybsteve, D. N.; Chun, H.; Yoon, S. H.; Kim, D.; Kim, K. *J. Am. Chem. Soc.* **2004**, *126*, 32.
- (29) Ferey, G.; Latroche, M.; Serre, C.; Millange, F.; Loiseau, T.; Percheron-Guegan, A. *Chem. Commun.* **2003**, 2976.
- (30) Dybsteve, D. N.; Chun, H.; Kim, K. *Angew. Chem., Int. Ed.* **2004**, *43*, 5033.
- (31) Pan, L.; Sander, M. B.; Huang, X.; Li, J.; Smith, M.; Bittner, E.; Bockrath, B.; Johnson, J. K. *J. Am. Chem. Soc.* **2004**, *126*, 1308.
- (32) Kubota, Y.; Takata, M.; Matsuda, R.; Kitagawa, S.; Kato, K.; Sakata, M.; Kobayashi, T. C. *Angew. Chem., Int. Ed.* **2005**, *44*, 920.
- (33) Antonelli, D. M. *Microporous Mesoporous Mater.* **1999**, *30*, 315.
- (34) He, X.; Antonelli, D. M. *Angew. Chem., Int. Ed.* **2002**, *41*, 214.
- (35) Kubas, G. J. *J. Organomet. Chem.* **2001**, *635*, 37.
- (36) Zhao, Yufeng; Kim, Yong-Hyun; Dillon, A. C.; Heben, M. J.; Zhang, S. B. *Phys. Rev. Lett.* **2005**, *94*, 155504.
- (37) Yildirim, T.; Ciraci, S. *Phys. Rev. Lett.* **2005**, *94*, 175501.
- (38) Hu, X.; Skadchenko, B. O.; Trudeau, M.; Antonelli, D. *J. Am. Chem. Soc.* **2006**, *128*, 11740.

- (39) Vettraiño, M.; Trudeau, M.; Antonelli, D. M. *Adv. Mater.* **2000**, *12*, 337.
- (40) Vettraiño, M.; Trudeau, M.; Antonelli, D. M. *Inorg. Chem.* **2001**, *40*, 2088.
- (41) He, X.; Trudeau, M.; Antonelli, D. *Adv. Mater.* **2000**, *12*, 1036.
- (42) He, X.; Trudeau, M.; Antonelli, D. *Inorg. Chem.* **2001**, *40*, 6463.
- (43) He, X.; Trudeau, M.; Antonelli, D. M. *Chem. Mater.* **2001**, *13*, 4808.
- (44) Fischer, E. O.; Reckziegel, A. *Chem. Ber.* **1961**, *94*, 2204.

The size of the sample chamber is 2.5 cm³. Lightly packed powder materials were used for all measurements. Before all measurements, the materials were degassed at 200 °C under a high vacuum for at least 1 day to remove any physisorbed water or volatile impurities. A simplified sketch of this apparatus is shown as follows



The temperature of the gas reservoir is measured by two AD590 IC thermometers that are calibrated against a standard mercury thermometer within 0.1 °C at room temperature. The sample temperature is measured with a type K thermocouple by converting voltage reading to temperature according to ITS-90 (The International Temperature Scale of 1990). The limits of error are 2 °C or 0.75% above 0 and 2 °C or 2% below 0 °C. The pressure of both gas reservoir and sample chamber is measured by Heise model HP0 pressure transducer, which has a full scale range of 1500 psi (about 100 atm). The accuracy of this transducer is rated to be 0.05% of the full scale, including nonlinearity, drift, and hysteresis. The GRC operates by admitting an appropriate amount of gas to the reservoir and determines its molar amount from its pressure and temperature. The system then manipulates the valves between the reservoir and the reaction chamber and transfers a desired amount of the gas from the reservoir to the gas reaction chamber. After equilibrium is attained, the system recalculates the number of hydrogen molecules. The number missing from the gas phase corresponds to the number of molecules absorbed by the sample. The system employs a modified Benedict–Webb–Rubin equation of state in calculating the amount of absorbed hydrogen from the pressure, temperature, and volume. The apparatus gradually increases the hydrogen pressure to the maximum specified value, while summing the sorbed hydrogen. The amount of hydrogen released from the sample is then determined by pumping out the gas reservoir and gradually bleeding hydrogen from the sample chamber into the gas reservoir. During the test process, the sample chamber was immersed in liquid nitrogen, and the liquid level was maintained.

This apparatus effectively measures the pressure of the hydrogen in the sample chamber and then calculates the number of moles on the basis of this pressure, the temperature, and the volume, which is arrived at by subtracting the sample volume (obtained by direct input of the sample weight and density) from the empty chamber volume. If the density used is the skeletal density measured by a pycnometer, the compressed hydrogen within the pores is treated as part of the sample chamber volume, but if the apparent density of the sample is used instead, the compressed gas in the pores is treated as having been absorbed by the sample along with the hydrogen physisorbed to the walls of the skeletal structure. The advantage of this system is that it eliminates the need to make assumptions on the void space volume of the material to obtain the total amount of H₂ in the system (including the compressed gas in the void space), which is crucial in determining the amount of useful fuel stored in the material. Most other Sieverts apparatus work by automatically subtracting out the compressed gas in the pores, obviating the use of the pycnometer, but making determination of the compressed gas in the pores more ambiguous. Gravimetric adsorption (equivalent to what is often called “excess storage”) and total storage are measured directly, whereas volu-

metric densities for both values are calculated using the apparent densities.

Enthalpies of adsorption were calculated using a variant of the Clausius–Clapeyron equation taking both the 77 and 87 K hydrogen adsorption data.

$$\ln\left(\frac{P_1}{P_2}\right) = \Delta H_{\text{ads}} \frac{T_2 - T_1}{RT_1 T_2} \quad (1)$$

where P_n = pressure for isotherm n , T_n = temperature for the isotherm n , and R = gas constant.

Pressure as a function of the amount adsorbed was determined by using exponential fit for each isotherm; the first 10 points of the isotherms were picked up and fit to the exponential equation. This exponential equation gives an accurate fit over the pressure up to 10 atm with the goodness of fit (R^2) above 0.99. The corresponding P_1 and P_2 values at a certain amount of H₂ adsorbed at both temperatures can be obtained by the simulated exponential equation. Inputting these numbers into the eq 1, we then calculated the enthalpies of the adsorption.

Synthesis. *Synthesis of Microporous Titanium Oxide Materials.* In a typical preparation, titanium(IV) isopropoxide (15 g, 52.77 mmol) was warmed with hexylamine (2.67 g, 26.39 mmol) until a homogeneous colorless solution was obtained. To this solution was added 75 mL of water with stirring. Precipitation occurred immediately. HCl (37%, 0.2603 g, 2.639 mmol) was then added to the mixture. The mixture was allowed to sit at room temperature overnight without agitation before being transferred to an oven for aging at 40 °C for 2 days, 60 °C for 2 days, and 80 °C for 4 days. The suspension was then filtered by suction filtration, and the white solid was placed into a sealed tube and put into an oven at 100 °C for 2 days, 120 °C for 2 days, and 140 °C for 2 days. The product was collected by suction filtration and washed once with a mixture of methanol (375 mL) and diethyl ether (125 mL) and four times with 500 mL of methanol. The resulting materials were put into an oven at 150 °C for 2 days.

Synthesis of Bis(benzene) and Bis(cyclopentadienyl) Transition-Metal-Reduced Microporous Titanium Oxides. Excess organometallic, as calculated on the basis of metal percent derived from the elemental analysis data (ca. 38% Ti), was added to a suspension of microporous titanium oxide in dry benzene under nitrogen. In a typical preparation, 1.0 g of the microporous solid is treated with 3.0 g of bis(benzene) chromium in 75 mL of benzene. After 2 days of being stirred to ensure complete absorption of the organometallic, the reduced material was collected by suction filtration under nitrogen and washed with successive 20-mL aliquots of benzene. The resulting materials were dried in vacuo at 1×10^{-3} Torr on a Schlenk line until all volatiles had been removed.

Results and Discussion

Bis(benzene)-Chromium-Reduced Composites. When a sample of microporous Ti oxide (C6–Ti), was treated with excess bis(benzene) chromium with respect to Ti in dry benzene over several days under nitrogen, a new black material (Bisben Cr–Ti) formed. The XRD and nitrogen adsorption data shown in Table 1 indicate that the wormhole pore structure of this material was retained. The elemental analysis of Bisben Cr–Ti showed a change from 3.12% C and 1.36% H in the starting material to 13.56% C and 1.83% H in the product, with 5.4% Cr, as determined by inductively coupled plasma spectrometry (ICP). The increased percentage of C is consistent with a large degree of structural retention

Table 1. Nitrogen Adsorption and XRD Results of C6–Ti Materials

sample	BET surface area (m ² /g)	BJH pore volume (cm ³ /g)	<i>d</i> -space of XRD (Å)
C6–Ti	941	0.673	25
Bisben Cr–Ti	404	0.192	25
Bisben V–Ti	243	0.143	25
Biscp Cr–Ti	461	0.299	25
Biscp V–Ti	513	0.337	25

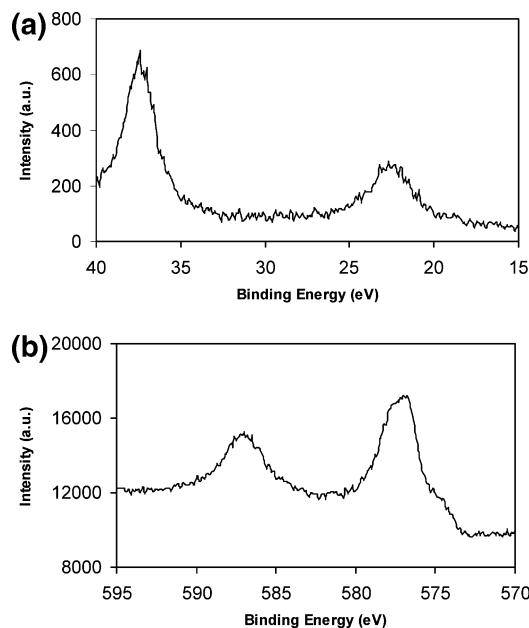


Figure 1. XPS spectrum of microporous titanium oxide treated with excess bis(benzene) chromium (Bisben Cr–Ti) showing the (a) Ti 3p 1/2, 3/2 and (b) Cr 2p 1/2, 3/2 regions.

for the bis(benzene) chromium complex without loss of the benzene rings.

To further probe the nature of the surface species present, we conducted X-ray photoelectron spectroscopy (XPS) studies. This is an effective technique for elucidating the different species present in the sample and the degree of reduction of the transition metal oxide framework.³⁹ Figure 1a shows the Ti 3p 1/2, 3/2 region of the XPS spectrum of Bisben Cr–Ti. The position of the Ti 3p 1/2 at 37.4 eV as compared to 37.9 eV in the unreduced material, is consistent with reduction of the Ti center by bis(benzene) chromium. This gradual shift to lower binding energy on reduction of the framework has been commented on before.^{41,42} These emissions are also broader than those in the starting material, as is the O 1s peak, providing further evidence for reduction of the Ti framework by bis(benzene) chromium. The Cr 2p 3/2, 1/2 region of the spectrum is shown in Figure 1b and shows major peaks at 577 and 586.8 eV; these emissions fall between those for neutral (C₆H₆)₂Cr at 575.7 and 584.8 eV and cationic species [(C₆H₆)₂Cr]⁺ with emissions at 577.7 and 586.7 eV.⁴⁵ These data are consistent with the existence of mixed-oxidation-state phases within the pores of the structure. The exact ratio Cr⁰/Cr^I is difficult to determine because of the low loading level of Cr and the sensitivity of the XPS technique.

Hydrogen pressure–composition isotherms were recorded at 77 K for pristine microporous Ti oxide (C6–Ti) and

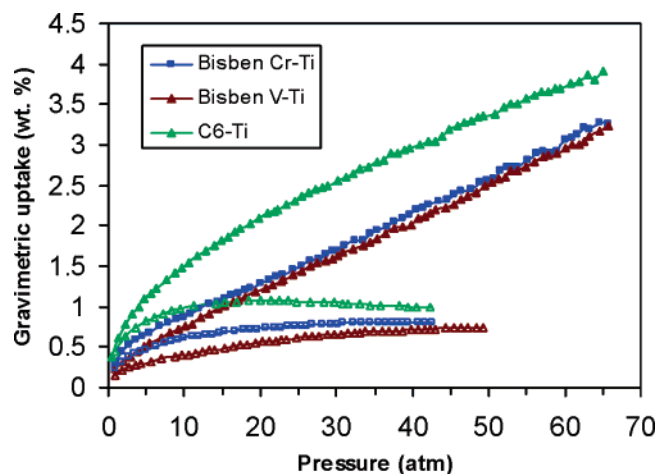


Figure 2. Gravimetric high-pressure H₂ isotherms for C6–Ti, Bisben Cr–Ti, and Bisben V–Ti at 77 K. Filled markers represent storage capacity and open markers denote adsorption capacity.

Bisben Cr–Ti. Both H₂ storage and adsorption isotherms are shown in Figure 2. The adsorption values reflect the amount of hydrogen bound to the surface of the porous framework, whereas the storage is a measure of the total H₂ available as fuel in any system (i.e., the sum of the adsorption and the compressed gas in the pores). These results and all other hydrogen sorption results in this study are summarized in Table 2, complete with extrapolation to 100 atm. Previous results for excess bis(toluene) titanium-reduced C6–Ti (BTTi C6–Ti), Li–naphthalene-reduced C6–Ti (Li C6–Ti), and Na–naphthalene-reduced C6–Ti (Na C6–Ti), as well as carbon AX-21, are also shown for comparison.³⁸ From Figure 2, we can see that all the storage isotherms rise sharply at low pressure and continue to rise in a linear fashion from 10 atm onward to 65 atm. Reversibility was evaluated by measuring the desorption branch down to near 0 atm. The desorption branches follow the adsorption branches without significant hysteresis. The adsorption/desorption process is fast and thermodynamic equilibrium was reached within a few seconds, indicating a very low activation barrier for this process. For the adsorption isotherms, the hydrogen capacity increases with increasing pressure until saturation is achieved, after which the hydrogen capacity begins to drop, a typical feature of supercritical adsorption.⁴⁶ Extrapolating to 100 atm, a feasible pressure for a cryogenic storage tank, Bisben Cr–Ti yields a total storage capacity of 4.76 wt % and 31.61 kg/m³, compared with 5.36 wt % and 29.37 kg/m³ for C6–Ti. The adsorption shows a decrease from 1.08 wt % and 5.918 kg/m³ in C6–Ti to 0.81 wt % and 5.378 kg/m³. The increased volumetric storage capacity is possibly due to the reduced Ti centers in the framework, which are better able to π -back-bond to the H₂ ligands and thus increase the strength of binding to the surface.³⁸ However, compared to the BTTi C6–Ti, the improvement of performance on reduction is somewhat less dramatic. This can be explained by a number of factors. Bis(benzene) chromium is a weaker reducing agent than bis(toluene) titanium, which can be verified from the XPS binding energy of Ti 3p 1/2 of Bisben Cr–Ti and BTTi C6–

(45) Binder, H.; Elschenbroich, C. *Angew. Chem., Int. Ed.* **1973**, *12*, 659.

(46) Zhou, Y.; Feng, K.; Sun, Y.; Zhou, L. *Chem. Phys. Lett.* **2003**, *380*, 526.

Table 2. Hydrogen Sorption Capacities of C6-Ti Materials and AX-21

sample	surface area (m ² /g)	apparent density (g/mL)	skeletal density (g/mL)	gravimetric adsorption (wt %)	gravimetric H ₂ storage (wt %) ^a	volumetric adsorption (kg/m ³)	volumetric H ₂ storage (kg/m ³) ^a
C6-Ti	942	0.548	2.698	1.08	5.36	5.918	29.37
Li C6-Ti	499	0.556	2.508	0.71	5.63	3.948	31.30
Na C6-Ti	480	0.565	2.741	0.92	5.58	5.198	31.58
BTTi C6-Ti	208	0.819	2.835	1.14	4.94	9.337	40.46
AX-21	3225	0.328	2.103	4.19	11.96	13.75	39.23
Bisben Cr-Ti	404	0.664	2.793	0.81	4.76	5.378	31.61
Bisben V-Ti	248	0.711	2.846	0.74	4.70	5.261	33.42
Biscp Cr-Ti	461	0.635	2.632	1.01	4.80	6.413	30.49
Biscp V-Ti	513	0.612	2.510	0.93	4.95	5.692	30.30

^a Hydrogen storage measurement is at a temperature of 77 K and pressure of 65 atm extrapolated to 100 atm with goodness of fit (R^2) = 0.9963–0.9992.

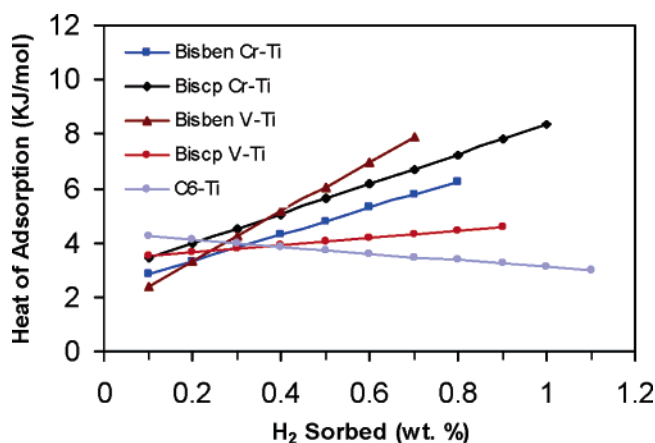


Figure 3. Enthalpy of H₂ adsorption for pristine and reduced microporous titanium oxides.

Ti.⁴⁷ Also, whereas bis(toluene) titanium completely loses its ligands to leave a thin layer of low-valence, low-coordinate Ti species on the surface of the pore channels,⁴⁷ bis(benzene) chromium leaves behind a mixture of the bis(benzene) chromium cation and the neutral species in the pores. Because of the coordinative saturation of these two Cr species, they are unable to contribute to hydrogen binding in the system. The decreased gravimetric storage capacity in Bisben Cr-Ti can be explained by the increased mass of the framework without a corresponding change in volume after treatment with the organometallic. From a gravimetric standpoint, it is clear that the increased framework will result in decreased gravimetric capacity. For some materials having very low density (such as activated carbon and MOFs materials), the high gravimetric density capacity can be obtained; however, the corresponding volumetric density will be low. For other materials, such as metal hydrides, the volumetric density can be very high because of the density of the material itself, but this comes with a tradeoff of a very low gravimetric density. These factors can thus account for the lower hydrogen sorption ability of Bisben Cr-Ti relative to that of BTTi C6-Ti.

The binding enthalpy of this material was calculated by a variant of the Clausius-Clayron equation⁴⁸ from hydrogen adsorption data at 77 and 87 K (see Figure 3). Because this is a complex solid with Ti $d_{xy}d_{xz}d_{yz}t_{2g}$ binding sites at and

below the surface of the pore channels, the enthalpies likely represent an average of many sites. The plot for this sample show an increase in ΔH with H₂ capacity, which is consistent with our previous results on reduced microporous titanias.³⁸ This highly unusual behavior may reflect a different mechanism of surface binding than simple physisorption, possibly involving a Kubas-type interaction. The maximum ΔH for Bisben Cr-Ti is 6.248 kJ/mol, somewhat lower than that for BTTi C6-Ti, reflecting the lower degree of surface reduction afforded by the weaker reducing agent.

Bis(benzene)-Vanadium-Reduced Composites. C6-Ti was treated with excess bis(benzene) vanadium⁴⁴ with respect to Ti in dry benzene for several days under nitrogen and the surface areas and pore volume of the resulting material (Bisben V-Ti) decreased as shown in Table 1, whereas XRD peak remained intact. This is consistent with occlusion of the pores of the microstructure by the encapsulated organometallic. The elemental analysis of Bisben V-Ti showed an increase in carbon from 3.12% in the starting material to 3.72% with 3.51% V as determined by ICP. The virtually unchanged C content in concert with the appearance of V indicates that the bis(benzene) vanadium loses its benzene ligands and deposits a small amount of an unsaturated vanadium species on the surface of the microstructure. This is similar to the action of bis(toluene) titanium; however, the addition of Ti to the composite and concomitant decomposition of the organometallic is autocatalytic at 60 °C and continues until the pores of the microstructure are completely blocked by low-valence Ti.

XPS studies were conducted for Bisben V-Ti. Figure 4a shows the Ti 3p region with the 1/2, 3/2 peaks in clear evidence. The position of the 3p 1/2 falls at 37.2 eV as compared to 37.4 eV in Bisben Cr-Ti and 37.9 eV in the unreduced material. This is fully consistent with reduction of the Ti center by bis(benzene) vanadium. In this case, the emission at 37.2 eV demonstrates reduction of the framework to a level of about Ti 3.3⁺. These emissions are also much broader than those in the starting material and Bisben Cr-Ti, providing further evidence for reduction of the Ti framework by bis(benzene) vanadium. Figure 4b shows the V 2p 3/2, 1/2 region, displaying two emissions at 515.3 and 523.3 eV, which can be assigned as V(II) species (515.6 and 523.2 eV).

Hydrogen pressure-composition isotherms at 77 K of both adsorption and storage for Bisben V-Ti are shown in Figure 2. This material yielded total storage values of 4.70 wt % and 33.42 kg/m³ in gravimetric and volumetric capacities,

(47) Vettrano, M.; Trudeau, M.; Lo, A. Y. H.; Schurko, R. W.; Antonelli, D. *J. Am. Chem. Soc.* **2002**, *124*, 9567.

(48) Roquerol, F.; Rouquerol, J.; Sing, K. *Adsorption by Powders and Solids: Principles, Methodology, and Applications*; Academic Press: London, 1999.

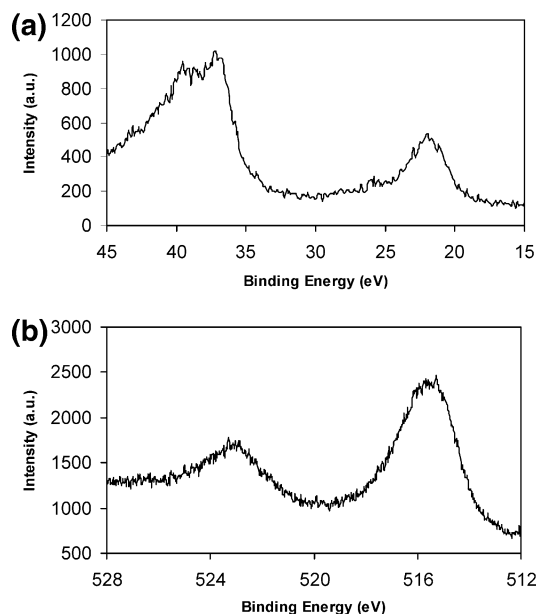


Figure 4. XPS spectrum of microporous titanium oxide treated with excess bis(benzene) vanadium (Bisben V-Ti) showing the (a) Ti 3p 1/2, 3/2 and (b) V 2p 1/2, 3/2 regions.

respectively. The overall increase in volumetric storage compared with Bisben Cr-Ti can be attributed to the stronger reducing ability of bis(benzene) vanadium than that of bis(benzene) chromium. Although the drop in gravimetric capacity is possibly due to the increased framework mass and lower surface area of Bisben V-Ti compared with Bisben Cr-Ti, many factors, including framework density, surface properties, and pore volume, are expected to be at play. The gravimetric and volumetric adsorption data for this material were 0.74 wt % and 5.261 kg/m³, respectively. The binding enthalpy of this material as a function of surface coverage is shown in Figure 3. As with other reduced microporous Ti oxides in this study, the enthalpy increases with the H₂ capacity. The maximum ΔH for Bisben V-Ti is 7.885 kJ/mol.

Bis(cyclopentadienyl)-Chromium-Reduced Composites.

C6-Ti was treated with excess bis(cyclopentadienyl) chromium with respect to Ti in dry benzene over several days under nitrogen, and a new black material (Biscp Cr-Ti) was formed. The XRD and nitrogen adsorption data shown in Table 1 indicate that the wormhole pore structure of this material was retained, with a reduction in pore volume and surface area. The elemental analysis of Biscp Cr-Ti showed an increase from 3.12% C and 1.36% H in the starting material to 13.68% C and 1.61% H in the product, with 5.81% Cr, as determined by ICP. The increased percentage of C is consistent with retention of the structural integrity of the organometallic without decomposition to chromium metal or chromium oxide. The Ti 3p 1/2, 3/2 regions of the X-ray photoelectron spectrum (XPS) of Biscp Cr-Ti are shown in Figure 5a. This spectrum exhibits a peak at 37.0 eV for Ti 3p 1/2 region. This gradual shift to lower binding energy, as compared to 37.9 eV in the unreduced material, is fully consistent with reduction of the Ti center by bis(cyclopentadienyl) chromium. The Cr 2p 1/2, 3/2 regions of the XPS (Figure 5b) show emissions at 586.5 and 577.1 eV, respectively. These numbers fall between the neutral bis-

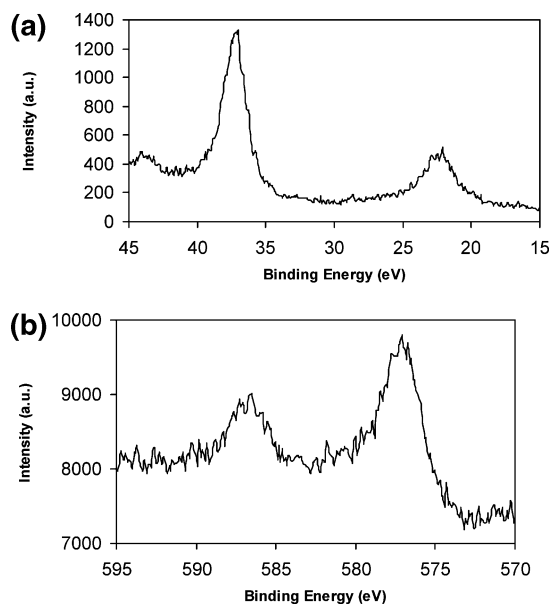


Figure 5. XPS spectrum of microporous titanium oxide treated with excess bis(cyclopentadienyl) chromium (Biscp Cr-Ti) showing the (a) Ti 3p 1/2, 3/2 regions. (b) Cr 2p 1/2, 3/2 regions.

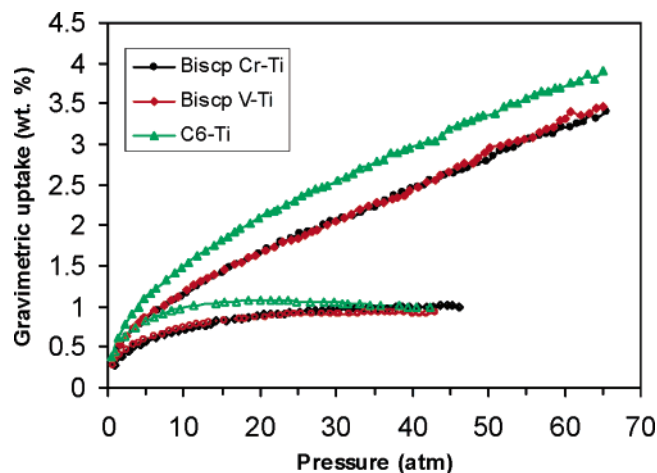


Figure 6. Gravimetric high-pressure H₂ isotherms for C6-Ti, Biscp Cr-Ti, and Biscp V-Ti at 77 K. Filled markers represent storage capacity and open markers denote adsorption capacity.

(cyclopentadienyl) Cr with peaks at 584.5 and 574.8 eV, a Cr (II) species having emissions at 585.5 and 575.7 eV, and a higher oxidation state Cr (IV) species with peaks at 587.1 and 577.4 eV, consistent with our previous results with the analogous Nb composites.⁴³

The hydrogen storage and adsorption isotherms of Biscp Cr-Ti are recorded in Figure 6, together with C6-Ti. From Figure 6, we can see the isotherms for this sample have the same trend with those of unreduced materials and the Ti and V bis(arene) transition-metal-reduced materials discussed above. The gravimetric and volumetric storage capacities for this sample are 4.80 wt % and 30.49 kg/m³, respectively. These results are similar to those recorded for Bisben Cr-Ti. However, Biscp Cr-Ti possesses a gravimetric adsorption of 1.01 wt % and a volumetric adsorption capacity of 6.413 kg/m³, which is higher than those of Bisben Cr-Ti. The reason for this could be the higher surface area as compared to that of Bisben Cr-Ti. As with Bisben Cr-Ti and Bisben V-Ti, an increase in binding enthalpy with surface coverage

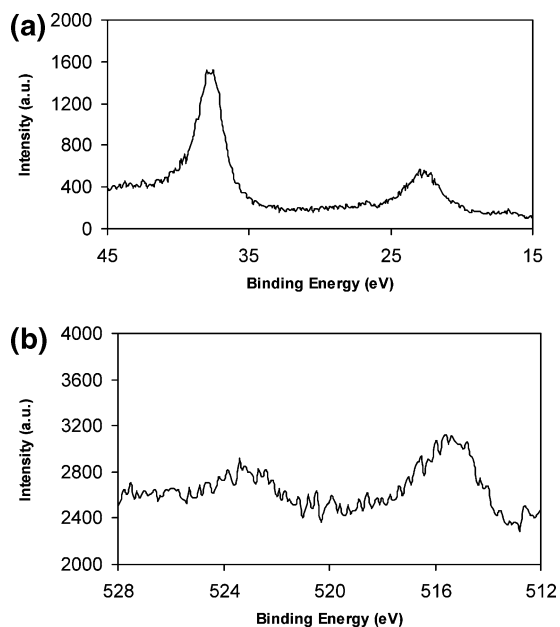


Figure 7. XPS spectra of microporous titanium oxide treated with excess bis(cyclopentadienyl) vanadium (Biscp V–Ti) showing the (a) Ti 3p 1/2, 3/2 and (b) V 2p 1/2, 3/2 regions.

was observed for this sample (Figure 3), with a maximum ΔH of 8.353 kJ/mol.

Bis(cyclopentadienyl) Vanadium Reduced Composites. C6–Ti was treated with excess bis(cyclopentadienyl) vanadium with respect to Ti in dry benzene for several days under nitrogen. The surface areas and pore volume of the resulting material (Biscp V–Ti) decreased as shown in Table 1, whereas the XRD peak remained intact. The elemental analysis of Biscp V–Ti showed an increase in carbon from 3.12% C and 1.36% H in the starting material to 11.26% C and 1.56% H with 3.53% V, as determined by ICP. The increase in carbon is fully consistent with retention of the structure of the bis(cyclopentadienyl) complex without loss of the organic rings. Figure 7a shows the XPS Ti 3p regions, with the 1/2 and 3/2 emissions in clear evidence. The position of Ti 3p 1/2 emission is 37.5 eV is consistent with reduction of Ti framework as compared described above. The slightly higher position of Ti 3p 1/2 emission as compared to the analogous bis(benzene) vanadium composite confirmed that bis(cyclopentadienyl) vanadium is a less effective reducing agent than the bis(benzene) vanadium. The V 2p 3/2 and 1/2 regions of the XPS (Figure 7b) show emissions at 515.6 and 524.3 eV, respectively. This can be assigned to a mixture of the neutral bis(cyclopentadienyl) vanadium species (513.0 and 520.2 eV), a vanadium(IV) species (514.9 and 522.4 eV), and a vanadium(V) species (516.4 and 524.5 eV).^{43,49}

Hydrogen storage and adsorption isotherms for Biscp V–Ti were recorded at 77 K and are shown in Figure 6. A gravimetric storage capacity of 4.95 wt % and volumetric storage capacity of 30.30 kg/m³ were obtained, respectively. The highest surface area of Biscp V–Ti in all these reduced materials in this study can attribute to the highest gravimetric capacity of reduced materials in this study, whereas the smallest apparent and skeletal density combined with the less-

reduced framework can explain its lowest volumetric capacity. The adsorption data showed a gravimetric capacity of 0.93 wt % and a volumetric capacity of 5.692 kg/m³. The H₂ binding enthalpy of Biscp V–Ti was shown at Figure 3. The plot still showed an increase in ΔH with H₂ capacity, which is typical for all the reduced samples in this and our previous study.³⁸ The maximum ΔH of Biscp V–Ti was 4.574 kJ/mol, which is the lowest of all reduced materials in this study.

Discussion

The most surprising trend in this series of materials is the seemingly small dependence on surface area of the gravimetric and volumetric adsorption or storage values. In general, cryogenic hydrogen storage values depend almost exclusively on surface area and pore structure in porous carbons and MOFs. In these materials, greater surface area and lower skeletal density usually lead to higher gravimetric storage values, whereas lower densities also lead to lower volumetric storage values. The fact that the best-performing material in our series has the lowest surface area (BTTi C6–Ti) clearly indicates that other factors are at play. Long et al. have demonstrated the effect of transition-metal linker on the adsorption values, in particular an anomalous adsorption trend involving a possible Kubas interaction with a Mn center.⁵⁰ In our materials, the evidence suggests that surface reduction has a greater effect on the performance than surface area or pore size. There is also an unusual trend in enthalpies, which show an increase in binding strength as the surface coverage increases. This is the opposite of all other cryogenic hydrogen storage materials, which show a small decrease with increasing surface coverage. As the surface becomes more crowded with hydrogen molecules, the effect of intermolecular repulsion becomes more important and begins to offset the van der Waals forces between the molecule and surface. An increase in binding enthalpy on surface coverage can only be explained in terms of the hydrogen molecules chemically or electronically modifying the surface, such that the surface interactions with subsequent hydrogen molecules are strengthened. Because hydrogen binding to transition metals normally increases with increased electron density at the metal, it is fair to suggest that increased surface coverage leads to an increased electron richness at the metal center due to σ -donation of the electrons in the H–H bonding orbital to the Ti centers. The increased electron density at the metal then leads to more effective π -back-donation to the antibonding H–H orbital and hence higher binding enthalpies. Although this is still speculative and other effects may be at play, it is difficult to verify any mechanism without in situ spectroscopic studies at low temperature, which are experimentally challenging because of the requirement of high hydrogen pressures and cryogenic temperatures in the sample cell.

In terms of increased storage values, it is clear from our data that surface reduction leads to an increase in density, with a concomitant increase in volumetric storage capacity. The gravimetric capacities are relatively unaffected, because

(49) *Handbook of X-ray Photoelectron Spectroscopy: Physical Electronics Division, Perkin-Elmer Corp.: Eden Prairie, MN.*

(50) Dinca, M.; Yu, A. F.; Long, J. R. *J. Am. Chem. Soc.* **2006**, *128*, 8904.

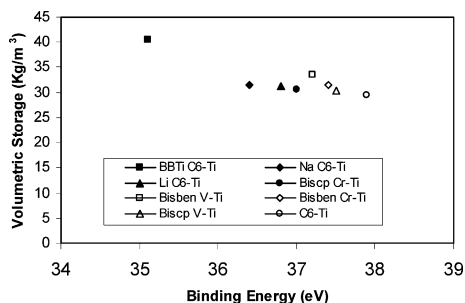


Figure 8. Plot of XPS Ti 3p 1/2 binding energy vs the hydrogen volumetric storage capacity for all the samples in this study and reduced samples from ref 38.

any increase in hydrogen binding is offset by an increase in density. A plot of XPS Ti 3p 1/2 binding energy versus hydrogen volumetric storage of all the samples in this study and the reduced samples at our previous study³⁸ is shown in Figure 8. This XPS emission has been used in previous work by our group to establish the oxidation state of the Ti centers in meso- and microporous Ti oxides. This figure shows a roughly linear, albeit empirical, relationship between the volumetric storage capacity and the degree of reduction of the microframework. Ascribing a precise meaning to this trend is difficult because of the complex interplay of often offsetting parameters, including (a) different skeletal densities that increase according to amount of reductant, (b) different surface areas, (c) different void space volumes that change with surface area as well as volume occupied by the counterion (i.e., Na, Li, (benzene)₂ chromium, etc.) and its respective solvation sphere, (d) different binding capacities as determined by degree of surface reduction of these materials, (e) different degrees of accessible coordinative unsaturation at the surface Ti or dopant sites, and (f) different capacities of Ti, V, or Cr to back-donate to H₂ depending on reduction level and Z_{eff}. Calculations by Zhao et al. indicate that zero-valence Sc should be the most effective at achieving an optimal binding interaction, with a trend toward decreased efficiency going to the right of the periodic table.³⁶ There is also the fact that some of the counterions (i.e., Na) are unable to bind hydrogen, but that the unsaturated Ti or V phase left by bis(toluenes) titanium or bis(benzene) vanadium is able to coordinate hydrogen. On top of this,

the enthalpies quoted in this work are clearly an average of many sites on the surface and beneath the surface of the walls of the amorphous microstructure (the walls are typically 15–20 Å thick and probably easily penetrated by the small hydrogen molecule). These facts aside, it is still clear that surface reduction has a dramatic effect on the volumetric storage capacities of these materials, even with the offsetting decrease in surface areas. Following the trend in Figure 8, it seems that even higher volumetric storage capacities are possible with more effective reducing agents that are better able to leave a low-valence surface, with a maximum degree of available coordinative unsaturation and lowest possible skeletal density.

Conclusion

In summary, in this study, a series of bis(benzene) and bis(cyclopentadienyl) transition-metal-reduced microporous titanium oxide composite materials were synthesized and characterized by nitrogen adsorption, XRD, XPS, and elemental analysis. The hydrogen sorption study at 77 K found that the gravimetric sorption capacities of these new reduced composites decreased compared with that of unreduced pristine samples, whereas the overall volumetric storage capacity increased. The unusual behavior of hydrogen binding enthalpies increasing with hydrogen sorption capacity were found for all the reduced samples, indicating a different sorption mechanism than simple physisorption possibly involving a Kubas-type interaction. The maximum hydrogen binding enthalpies for these new composites ranged from 4.57 to 8.35 kJ/mol, but still fell short of the 15 kJ/mol value proposed for porous materials to function effectively at ambient temperature. Further investigation is needed to find suitable reducing agents that can lead to greater storage capacity to meet goals set by the U.S. DOE and to achieve more precise control of the enthalpies to operate at more practical temperatures.

Acknowledgment. The authors acknowledge the Natural Science and Engineering Research Council of Canada for funding.

CM062933L